Journal of
Applied Remote Sensing

Crop classification using HJ satellite multispectral data in the North China Plain

Kun Jia
Bingfang Wu
Qiangzi Li

SPIE

Crop classification using HJ satellite multispectral data in the North China Plain

Kun Jia,[a,d] Bingfang Wu,[a,b,c] and Qiangzi Li[a,c]

[a]Beijing Normal University and the Institute of Remote Sensing and Digital Earth of Chinese Academy of Sciences, State Key Laboratory of Remote Sensing Science, Beijing 100875, China

[b]Chinese Academy of Sciences, Institute of Remote Sensing and Digital Earth, Key Laboratory of Digital Earth Science, Beijing 100094, China

wubf@irsa.ac.cn

[c]Chinese Academy of Sciences, Institute of Remote Sensing and Digital Earth, Beijing 100094, China

[d]Beijing Normal University, College of Global Change and Earth System Science, Beijing 100875, China

Abstract. The HJ satellite constellation is designed for environment and disaster monitoring by the Chinese government. This paper investigates the performance of multitemporal multispectral charge-coupled device (CCD) data on board HJ-1-A and HJ-1-B for crop classification in the North China Plain. Support vector machine classifier is selected for the classification using different combinations of multitemporal HJ multispectral data. The results indicate that multitemporal HJ CCD data could effectively identify wheat fields with an overall classification accuracy of 91.7%. Considering only single temporal data, 88.2% is the best classification accuracy achieved using the data acquired at the flowering time of wheat. The performance of the combination of two temporal data acquired at the jointing and flowering times of wheat is almost as well as using all three temporal data, indicating that two appropriate temporal data are enough for wheat classification, and much more data have little effect on improving the classification accuracy. Moreover, two temporal data acquired over a larger time interval achieves better results than that over a smaller interval. However, the field borders and smaller cotton fields cannot be identified effectively by HJ multispectral data, and misclassification phenomenon exists because of the relatively coarse spatial resolution. © *2013 Society of Photo-Optical Instrumentation Engineers (SPIE)* [DOI: 10.1117/1.JRS.7.073576]

Keywords: HJ satellite; multispectral; multitemporal; crop; classification.

Paper 12450 received Dec. 1, 2012; revised manuscript received Mar. 12, 2013; accepted for publication Mar. 15, 2013; published online Apr. 12, 2013.

1 Introduction

Remote sensing techniques have long been important means for agricultural monitoring, with their ability to quickly and efficiently collect information about spatial variability occurring in the field.[1,2] Crop identification is the main issue for agriculture monitoring using remote sensing techniques and the basis for crop acreage and production estimation, which are critical factors for many applications in the domain of agriculture.[3,4] Due to the complex natural environment and cropping systems, crop classification in China using remote sensing is much more difficult.[5] Previous researchers have indicated that the problem of misclassification still exists, even when using very high spatial resolution remote sensing data (such as QuickBird image).[6] Considering the large acreage and wide distribution of farmland in China, it is impossible for wall-to-wall monitoring of agriculture fields using high spatial resolution remote sensing data, thus the realistic substitutable data may be moderate spatial resolution data (about 30 m spatial resolution) with wide coverage ability.[7]

The HJ satellite constellation is designed mainly for environment and disaster monitoring by the Chinese government. As part of the HJ satellite constellation, two optical satellites (HJ-1-A

0091-3286/2013/$25.00 © 2013 SPIE

and HJ-1-B) are launched on September 6, 2008.[8] HJ satellite data is freely available to the public and operated by China Centre for Resources Satellite Data and Application, with the relevant information available at http://www.cresda.com/n16/n1115/n1432/index.html with the interface in Chinese. HJ-1-A and HJ-1-B carry two charge-coupled device (CCD) cameras with the same configuration, respectively, and distributed with a phase difference of 180 in the same orbital plane to enhance the temporal resolution of earth observations and to obtain mosaic images from the two satellites.[9] The CCD data has four spectral bands with a spectrum ranging from 430 to 900 nm and spatial resolution of 30 m.[10] The main sensors and their parameters for HJ-1-A/B are shown in Table 1. The multispectral information, moderate spatial resolution, and the large coverage capability of the HJ CCD data make it a highly suitable data source for agricultural monitoring on a regional scale. If microwave sensor data on board HJ-1-C satellite is available later, the HJ constellation will have large scale and all-weather imaging capability, which will be a powerful data source for earth observation. Therefore, exploring the application capability of HJ multispectral data in agricultural monitoring is a significant work.

Due to the limitations of technique and differences in work mechanisms, any single sensor data cannot fully characterize the land surface objects in the complex earth environment.[11,12] Optical sensors can provide spectral information in the reflective and thermal emissive portions of the electromagnetic spectrum. However, due to the limits of spectral resolution, spatial resolution, and number of wavebands, the identification ability of optical sensors is restricted seriously, especially for vegetation recognition, because the spectral characteristics of different vegetation are similar and difficult to classify. One of the major findings from various studies on remote-sensing-based crop monitoring is that maximum discrimination between different crop types occurs at different stages in the growth cycle, and capturing all these differences is not possible using a single-temporal image.[13] Consequently, multitemporal image data collected by repeated overpasses has been recommended to improve the discrimination accuracy.[14,15] Conese and Maselli compared the classification performance of single-temporal and multitemporal thematic mapper data and found that temporal information had greatly improved the classification accuracy.[16] Vieira and Mather proved that the accuracy of crop classification derived from multitemporal data was considerably higher compared with the accuracy obtained with single-temporal data.[17] Wang et al. used multitemporal Envisat ASAR data to map the agricultural area in the Pearl River Delta and proved multitemporal radar backscatter information received in the crop growth period was important in improving classification accuracy.[18] Therefore, it is necessary to investigate the capability of multitemporal HJ CCD data for crop classification.

The objective of this study is to investigate the capability of HJ CCD data and demonstrate their application potential for crop classification in the North China Plain. In addition, considering the limitations of a single data, multitemporal data of HJ CCD are also investigated for crop

Table 1 Technical specification of payloads on HJ-1-A/B.

Satellite	Payload	Band No.	Spectral range (μm)	Nadir spatial resolution (m)	Swath width (km)	Side looking ability (deg)	Repetition cycle (day)
HJ-1-A/B	Multispectral CCD camera	1	0.43–0.52	30	360 (700 for two)	/	4
		2	0.52–0.60				
		3	0.63–0.69				
		4	0.76–0.90				
HJ-1-A	Hyperspectral imager	/	0.45–0.95 (110–128 bands)	100	50	±30	4
HJ-1-B	Infrared multispectral camera	5	0.75–1.10	150	720	/	4
		6	1.55–1.75	150			
		7	3.50–3.90	150			
		8	10.5–12.5	300	8	8	8

classification. Significant research has been conducted on the multitemporal classification for agricultural monitoring, and a number of methods have been proposed for effective classification of multidimensional data.[13] In dealing with a finite dataset, minimizing the influence of the searching space dimension onto the classifier performance is important so that results depend only on the number of pieces of added information. Support vector machine (SVM),[19] a kernel-based supervised classifier, which is widely used for land cover classification using remote sensing data and performs better results,[20–24] is a suitable selection in this study, inherent computational cost notwithstanding.

2 Study Area and Field Survey

The North China Plain, with an area of approximately 300,000 km^2, is the second largest plain in China. Approximately 437 million people live in the North China Plain in 2000, accounting for 34.8% of China's total population.[25] The study area is located in Yucheng County (centered at 36 deg 47′N, 116 deg 33′E), Shandong Province, China (Fig. 1). This region belongs to the temperate climate zone and is a typical upland field agriculture area in the North China Plain. It is relatively flat farmland with an average altitude of about 20 m above the sea level, so that uncertainty of classification accuracy caused by topographical facts will be reduced to a minimum. The annual precipitation is about 582 mm, and the annual average temperature is about 13.1°C. The study area selected in this study is about 15×15 km. Though it is not a big region, it has the representative characters of crop type distribution in the North China Plain. The study area is planted mainly with winter wheat and a small quantity of cotton. Wheat season begins in early October, and the wheat is harvested in early June the following year. Cotton is planted in April and harvested in September.

In order to determine the actual crop distribution in the study area, a high spatial resolution RapidEye image was acquired in February 2009. For selection of training and validating samples and to assist the visual interpretation of RapidEye data, a field survey to identify the main classes in the study area was carried out on May 19, 2009. During the survey, the details of the representative land cover were recorded, and the position had been recorded with the help of a handheld global positioning system receiver with positioning accuracy approximately ± 5 m.

3 Data and Preprocessing

In this study, three HJ-1 CCD images were acquired during the growth periods of wheat in 2009 (Table 2). Cloud influence was not present, and the quality of the multispectral image was good. The HJ CCD image preprocessing included radiance calibration and geo-correction. The

Fig. 1 The pink square in the image shows the location of the Yucheng study area in Shandong Province.

Table 2 Main characteristics of the data sets used in this study.

Satellite	Sensor	Date (dd/mm/yy)	Periods of wheat	Simple code in this study
HJ-1-A	CCD2	28/03/2009	Jointing	HJ3
HJ-1-B	CCD2	26/04/2009	Before flowering	HJ4
HJ-1-B	CCD1	12/05/2009	Flowering	HJ5

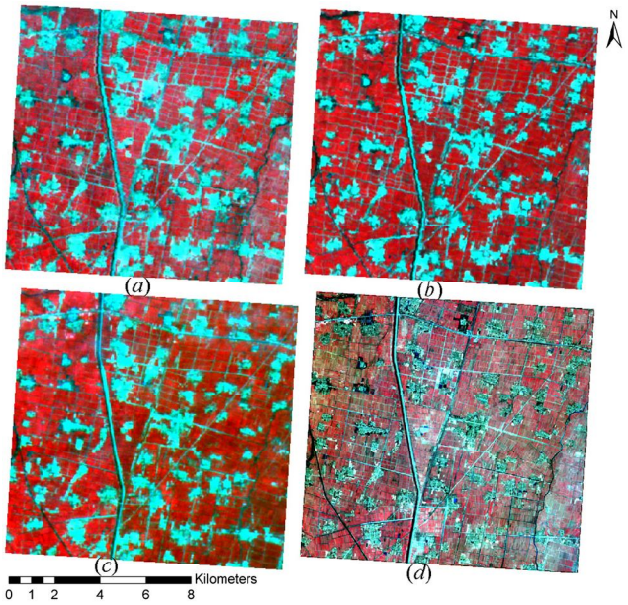

Fig. 2 Clipped images from satellite data obtained at different times. The NIR, red, and green bands were assigned to red, green, and blue color bands. Images are clipped from (a) HJ CCD false color image on March 28, 2009; (b) HJ CCD false color image on April 26, 2009; (c) HJ CCD false color image on May 12, 2009; and (d) RapidEye false color image on February 28, 2009.

radiance calibration of the HJ data was to convert the DN value of the raw image to surface spectral reflectance. Atmospheric correction was done using a 6S model,[26] and four wavebands surface spectral reflectance of the HJ CCD data were determined finally (Fig. 2).

A RapidEye multispectral data with 5-m spatial resolution was acquired on February 28, 2009 (Fig. 2). The RapidEye data was used mainly for ground surveys and visual interpretation to assist the selection of training and validating samples in the classification process.

Based on the knowledge of species distribution characteristics, four classes were identified as the final class types in this study: wheat, cotton, tree, and nonvegetated areas. Nonvegetated areas include residential areas, roads, water bodies, and bare land. Randomly selected sample pixels using the region of interest (ROI) tools provided by ENVI version 4.5 (ITT Industries Inc., Boulder, Colorado) based on the ground truth image obtained from visual interpretation of RapidEye image and ground survey as described above were used to train and validate the

Table 3 Number of regions of interest (ROIs) and pixels in each class type used for training and validating the support vector machine (SVM) classifier.

	Nonveg.	Tree	Cotton	Wheat
Number of ROIs	29	6	10	22
Number of pixels	552	82	94	580

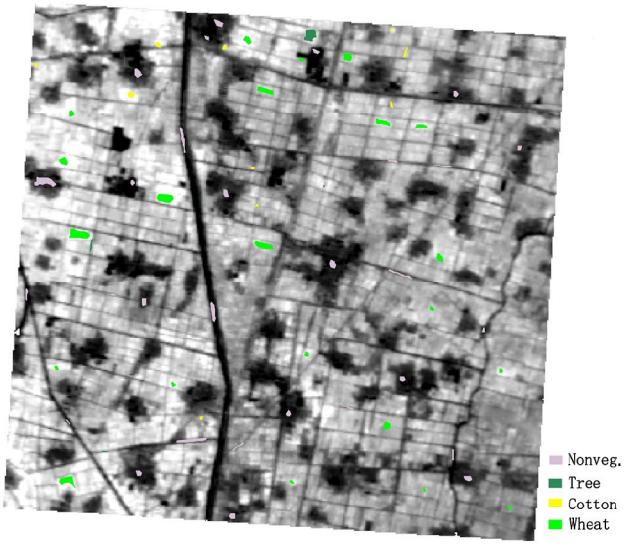

Fig. 3 The spatial distribution of samples used in this study. The gray image was the near infrared band from HJ multispectral data acquired on May 12, 2009.

classifier. Table 3 summarized the characteristics of the sample ROIs for training and validating the classifier, and Fig. 3 shows the spatial distribution of the selected ROIs. The sample pixels for wheat, cotton, and nonvegetated classes were always the pure pixels, except for some narrow cotton fields and some roads in the nonvegetated class. For the tree class usually being planted aside the road and having a narrow width compared with the spatial resolution of HJ data, its sample pixels were usually not pure, except for a square wood field found in the top center region of the study area (Fig. 3). The distribution of the sample pixels was uniform, which made it well representative for the whole study area. Half of the sample pixels were randomly selected as training samples, and the remaining half as validating samples. The training and validating samples had no overlap.

To evaluate the performance of HJ CCD multispectral data in crop classification, the classification results were compared with those produced by a visual interpretation of the RapidEye image. The objective was to determine whether the HJ CCD data had the potential for crop classification. Randomly selected sample pixels, as described above, were used to quantitatively validate the crop classification results. These homogeneous sample areas were identified easily on the HJ CCD and RapidEye image within the study area. The final sample pixels for classification accuracy estimation were: 276 pixels for nonvegetation, 290 for wheat, 47 for cotton, and 41 for trees. The overall classification accuracy, producer's accuracy, user's accuracy, and Kappa statistics were then estimated.[27–29]

4 Classification Method

The SVM classifier, which has been widely used for classification of remote sensing data, is selected for crop classification using HJ multispectral data in this study.[21,30,31] What follows is a brief introduction to the theory of SVM. The modern SVM is introduced by Cortes and Vapnik,[32] and a detailed description of the SVM can be found in Burges.[33] The SVM training algorithm promises to obtain the optimal separating hyper-plane for a training data set in terms of the generalization error. Given a set of examples $(x_i,\ y_i)$, $i = 1 \ldots l$ where $x_i \in R^n$ and $y_i \in \{-1, +1\}$, the SVM requires the solution to the following optimization problem, given in Eq. (1):

$$\min_{w,b,\xi}\left(\frac{1}{2}w^{\mathrm{T}} \cdot w + C\sum_{i=1}^{l}\xi_i\right) \quad \text{subject to } y_i \cdot (w^{\mathrm{T}} \cdot \Phi(x_i) + b) \geq 1 - \xi_i, \xi_i \geq 0, \tag{1}$$

where ξ_i is a slack variable and $C > 0$ is a preset penalty value for misclassification errors. The training vector x_i is mapped into a higher (maybe infinite) dimensional space by the function Φ. The $w^{\mathrm{T}} \cdot \Phi(x_i) + b$ is a hyper-plane in this higher dimensional space. The SVM method will then find an optimal separating hyper-plane. Furthermore, $k(x_i, x_j) = \Phi(x_i)^{\mathrm{T}} \cdot \Phi(x_j)$ is called the kernel function.

The choice of the kernel function k is crucial for good classification performance. In this study, the radial basis function (RBF) is used, as given in Eq. (2):

$$k(x_i, x_j) = \exp(-\gamma \cdot \|x_i - x_j\|^2), \qquad \gamma > 0 \tag{2}$$

Here, γ is a kernel parameter. The RBF is one of the most commonly used kernel functions. In general, the RBF is a reasonable choice. First, the RBF kernel nonlinearly maps samples into a higher-dimensional space, so the RBF can handle the case when the relationship between class labels and attributes is nonlinear. Second, the RBF kernel has fewer numerical computational difficulties. C and γ are the two parameters using RBF kernels. In this study, the C and γ parameters in kernel function are experiencedly set to 100 and 0.25, respectively.

The same training samples and parameters of classifiers are used for different combination of multitemporal HJ CCD data, which are ensured that different classification results are comparable.

5 Results

5.1 *Classification Results*

The classification results of HJ multispectral data and different combinations of these data were shown in Fig. 4. In the visual aspect, wheat fields could be identified effectively in each classification map, based on the ground survey and a visual interpretation of the RapidEye image. The main difference in the various classification results was the misclassification of field borders and identification of cotton and tree fields. In the classification result using only one temporal HJ CCD data, the data acquired at the flowering time of wheat (HJ5) performed better than the other two data. In the classification map of the HJ data acquired at the jointing time of wheat (HJ3), only a small portion of cotton fields was identified and mostly classified incorrectly into the nonvegetation class (the cotton had not yet sprouted during that period). However, in the classification map of data acquired before the flowering time of wheat (HJ4), many wheat pixels located in the field borders were misclassified as cotton pixels. The reason for this phenomenon was that the cotton was small seedlings during this period and had a small canopy coverage rate, and mixed pixels were seen in the borders of the wheat field due to the relatively coarse spatial resolution of the HJ CCD data, which led to the similar spectral characteristics of the cotton field and the mixed pixels in the wheat field borders.

In the classification result using multitemporal HJ CCD data, the classification performance improved as more temporal data was added for classification. When all the data acquired in this study were used for classification, the best performance was achieved. The wheat fields were identified correctly, and the misclassification was reduced to a minimum. The classification performance of HJ3 + HJ5 was nearly as well as that using all the three data and better than the other two combinations (HJ3 + HJ4 and HJ4 + HJ5). The reason might be that the plants showed a large change in their canopy structure and biochemical contents over a long time interval, and then a large difference in spectral characteristics of the crops formed and the spectral separability between different classes was enlarged.

However, in every classification map, cotton fields could not be discriminated from other species. The main reason might be that the cotton fields were usually rectangular with a narrow width (usually less than 10 m wide), and the phenomena of cotton planted under trees commonly occurred, which made the HJ CCD data with 30 m spatial resolution have no advantages in identifying narrow cotton fields. At the same time, the identification of field borders using HJ data was also not well. Many field borders were not discriminated from other classes.

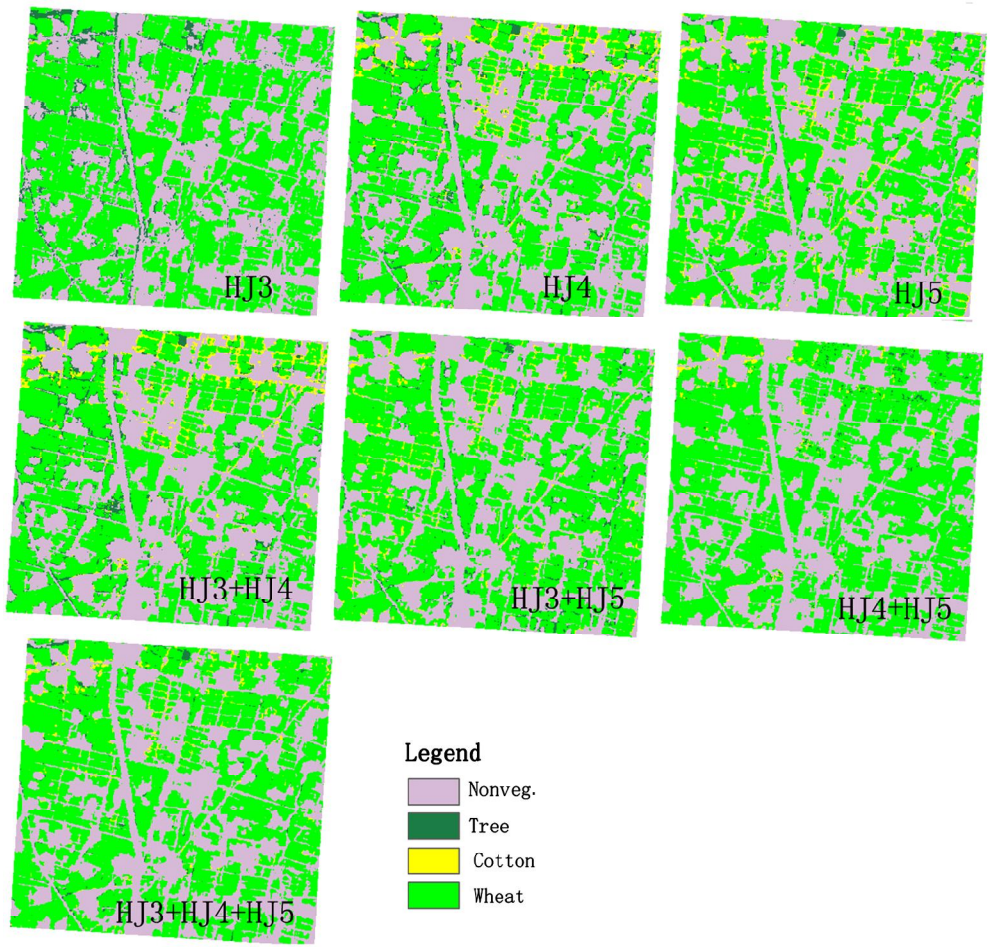

Fig. 4 Classification results using the HJ CCD data and different combinations of these multitemporal data. The meaning of the sample code in the lower right of each classification map is found in Table 2 (i.e., HJ3 means the HJ CCD data was acquired in March of 2009, and HJ3 + HJ4 means the classification was done using a combination of HJ3 and HJ4 data).

5.2 *Accuracy Validation*

The classification accuracy and kappa statistics were estimated based on the validating samples (Table 4). The overall classification accuracies using different combinations of HJ CCD data were all more than 80%, especially the classification accuracy using three temporal HJ CCD data that reached the highest overall classification accuracy of 91.7% and a kappa value of 0.87, which was an acceptable accuracy for crop monitoring. The overall classification accuracy of HJ5 (88.2%) was better than HJ3 (82.7%) and HJ4 (85.8%). This indicated that the flowering period of wheat was more suitable for crop classification than the other two periods.

It was too early for crop-type identification during the jointing period of wheat because the cotton had not yet germinated, which also could be seen from the producer and user accuracy of the HJ3 classification results when confusion between cotton and nonvegetation pixels was evident. The performance of HJ4 was better than HJ3 but slightly worse than HJ5.

In the classification results using two temporal HJ CCD data, HJ3 + HJ5 (overall classification accuracy of 90.8% and kappa value of 0.85) performed better than the other two combinations, which provided the same results as the visual observation. The performance of HJ3 + HJ4 (overall classification accuracy of 86.4% and kappa value of 0.77) was worst in the three combinations, which indicated that the data acquired during the late growth periods of wheat was more important for crop classification. The performance using the three temporal data was only slightly improved compared with the combination of HJ3 and HJ5, less than one percentage in overall classification accuracy. It indicated that two appropriate temporal HJ CCD

Table 4 Evaluation of crop classification performance using HJ CCD data and different combination of multitemporal HJ CCD data by SVM classifier.

Combination of HJ data	Overall accuracy	Kappa	Class type	Producer accuracy	User accuracy
HJ3	82.7	0.7	Nonveg.	86.96	87.27
			Tree	46.34	65.52
			Cotton	2.13	100.00
			Wheat	96.90	80.52
HJ4	85.8	0.76	Nonveg.	92.75	90.14
			Tree	39.02	84.21
			Cotton	27.66	46.43
			Wheat	95.17	85.45
HJ5	88.2	0.8	Nonveg.	95.65	98.51
			Tree	41.46	89.47
			Cotton	31.91	75.00
			Wheat	96.90	80.98
HJ3 + HJ4	86.4	0.77	Nonveg.	93.48	88.36
			Tree	39.02	100.00
			Cotton	31.91	53.57
			Wheat	95.17	86.79
HJ3 + HJ5	90.8	0.85	Nonveg.	96.38	96.38
			Tree	60.98	69.44
			Cotton	76.60	69.23
			Wheat	92.07	92.07
HJ4 + HJ5	89.3	0.82	Nonveg.	96.38	95.68
			Tree	53.66	88.00
			Cotton	38.30	66.67
			Wheat	95.86	85.8
HJ3 + HJ4 + HJ5	91.7	0.87	Nonveg.	96.01	97.79
			Tree	63.41	72.22
			Cotton	87.23	75.93
			Wheat	92.41	91.47

data contained enough information for wheat and cotton classification, and more temporal data had little help for improving classification performance.

6 Discussions and Conclusions

HJ multispectral data is an attractive data source for agriculture monitoring in large regions for its large region-imaging capability and moderate spatial resolution. The investigation of crop

classification using HJ multispectral data in the North China Plain indicated that it is an effectively data source. HJ multispectral data could effectively classify wheat fields, and the overall classification accuracy reached 91.7% using multitemporal data with an SVM classifier, but the smaller cotton fields and field borders could not be recognized effectively. The main reason for this phenomenon was the moderate spatial resolution of HJ multispectral data and the complex land surface. The spatial resolution of HJ multispectral data was 30 m, which was very low for identification of field borders. Furthermore, cotton fields were usually a rectangle with a narrow width (usually less than 10 m), and the phenomena of cotton planted under trees commonly existed, all of which led to cotton field misclassification using the relatively coarse spatial resolution HJ multispectral data.

In the North China Plain, winter wheat was the major crop type in the summer growth season, and the fields were large, which accounted for more than 90% of the farmland in this study. Cotton was planted less, and the field sizes were also smaller compared with the spatial resolution of HJ multispectral data. Therefore the classification of wheat tended to have a higher accuracy, whereas the classification accuracy of cotton tended to be lower. This phenomenon could be observed from the overall classification accuracy, user, and producer accuracy from Table 4. Thus if more detailed information about the cotton cultivation, much higher spatial resolution remote sensing data was needed, the spatial resolution of HJ multispectral data was not enough for small cotton fields identification.

Considering the classification performance using single-temporal HJ multispectral data, the data acquired at the flowering period of wheat performed better than the other two periods, and the data acquired at the jointing period performed worst. The reason might be that cotton had not germinated at the jointing period of wheat, which resulted in similar spectral characteristics of cotton fields with bare land and unsurfaced roads on the HJ multispectral data, and they could not be identified based on spectral differences. However, at the flowering period, wheat was much taller (about 70 cm) and had almost 100% surface coverage, which greatly influenced the electromagnetic signal of the HJ multispectral data and resulted in different spectral characteristics between wheat and cotton and other classes. The classification results indicated that flowering time was the most important period for wheat and cotton classification using HJ multispectral data during the three growing periods of wheat.

When considering the multitemporal HJ multispectral data, the combination of all three temporal data achieved the best classification accuracy (91.7%), which indicated that using more temporal HJ multispectral data could provide more information for crop classification. If using only two temporal HJ multispectral data for classification, the combination of data acquired at jointing and flowering periods performed better than the other two combinations. It is indicated that two temporal data acquired over a larger time interval performed better than data acquired over a smaller interval. This was because the crops had large changes in their canopy structure and in the biochemical contents over a long time interval, and then a large difference in spectral characteristics of the crops formed and the spectral separability was enlarged. In addition, the performance of this combination was almost as well as using all three temporal data. Overall, the information contained in two temporal HJ multispectral data, if acquired at the appropriate time, were enough for wheat classification. More temporal data brought information redundancy, which had little effect on improving classification accuracy. This phenomenon was also observed by Shao when she investigated rice monitoring using multitemporal Radarsat data in the Zhaoqing area.[15] She also found that only three temporal radar data acquired at the end of the transplanting and seedling development period, during the ear differentiation period, and at the beginning of the harvest period of rice were enough for rice production estimation.

From this study, the following conclusions were made: (1) HJ multispectral data could effectively classify winter wheat fields in the North China Plain, but field borders and smaller cotton fields could not be recognized effectively and would be misclassified; (2) more temporal HJ multispectral data contained more information for crop classification, and the data acquired during late growth periods of wheat performed better; (3) two temporal data acquired over a larger time interval performed better than data acquired over a smaller interval; (4) two appropriate temporal HJ multispectral data had been shown sufficient for winter wheat classification in this study, and additional temporal data had almost no effect on improving classification accuracy. In this study, only multispectral data of HJ satellite was investigated for crop classification.

Hyperspectral data on board HJ-1-A and microwave sensor on board HJ-1-C were also the potential data sources for crop classification, and investigation of these data would be done in the future.

Acknowledgments

The work in this paper was supported by the National High Technology Research and Development Program of China (863 Program) (No. 2012AA12A307) and the Key Research Program of the Chinese Academy of Sciences (No. KZZD-EW-08-05). The authors also thank Eastdawn Corporation for providing the RapidEye data in this study.

References

1. M. C. González-Sanpedro et al., "Seasonal variations of leaf area index of agricultural fields retrieved from Landsat data," *Remote Sens. Environ.* **112**(3), 810–824 (2008), http://dx.doi.org/10.1016/j.rse.2007.06.018.
2. K. Jia et al., "Vegetation classification method with biochemical composition estimated from remote sensing data," *Int. J. Remote Sens.* **32**(24), 9307–9325 (2011), http://dx.doi.org/10.1080/01431161.2011.554454.
3. B. F. Wu, "Operational remote sensing methods for agriculture statistics," *Acta Geograph. Sin.* **55**(1), 23–55 (2000) (in Chinese with English abstract).
4. M. Zhang et al., "Crop discrimination in Northern China with double cropping systems using Fourier analysis of time-series MODIS data," *Int. J. Appl. Earth Obs. Geoinform.* **10**(4), 476–485 (2008), http://dx.doi.org/10.1016/j.jag.2007.11.002.
5. B. Wu and Q. Li, "Crop planting and type proportion method for crop acreage estimation of complex agricultural landscapes," *Int. J. Appl. Earth Obs. Geoinform.* **16**, 101–112 (2012), http://dx.doi.org/10.1016/j.jag.2011.12.006.
6. B. Wu et al., "QuickBird imagery for crop pattern mapping," *J. Remote Sens.* **8**(6), 688–695 (2004) (in Chinese with English abstract).
7. Q. Li et al., "Maize acreage estimation using ENVISAT MERIS and CBERS-02B CCD data in the North China Plain," *Comput. Electron. Agr.* **78**(2), 208–214 (2011), http://dx.doi.org/10.1016/j.compag.2011.07.008.
8. H. Guo, "China's earth observing satellites for building a digital earth," *Int. J. Dig. Earth* **5**(3), 185–188 (2012), http://dx.doi.org/10.1080/17538947.2012.669960.
9. Q. Wang et al., "Chinese HJ-1A/B satellites and data characteristics," *Sci. China Earth Sci.* **53**(1), 51–57 (2010), http://dx.doi.org/10.1007/s11430-010-4139-0.
10. J. Chen, J. Huang, and J. Hu, "Mapping rice planting areas in southern China using the China environment satellite data," *Math. Comput. Model.* **54**(3–4), 1037–1043 (2011), http://dx.doi.org/10.1016/j.mcm.2010.11.033.
11. X. Blaes, L. Vanhalle, and P. Defourny, "Efficiency of crop identification based on optical and SAR image time series," *Remote Sens. Environ.* **96**(3–4), 352–365 (2005), http://dx.doi.org/10.1016/j.rse.2005.03.010.
12. K. Jia et al., "Crop classification using multiconfiguration SAR data in the North China Plain," *Int. J. Remote Sens.* **33**(1), 170–183 (2012), http://dx.doi.org/10.1080/01431161.2011.587844.
13. C. S. Murthy, P. V. Raju, and K. V. S. Badrinath, "Classification of wheat crop with multitemporal images: performance of maximum likelihood and artificial neural networks," *Int. J. Remote Sens.* **24**(23), 4871–4891 (2003), http://dx.doi.org/10.1080/0143116031000070490.
14. T. Le Toan et al., "Rice crop mapping and monitoring using ERS-1 data based on experiment and modeling results," *IEEE Trans. Geosci. Remote Sens.* **35**(1), 41–56 (1997), http://dx.doi.org/10.1109/36.551933.
15. Y. Shao et al., "Rice monitoring and production estimation using multitemporal RADARSAT," *Remote Sens. Environ.* **76**(3), 310–325 (2001), http://dx.doi.org/10.1016/S0034-4257(00)00212-1.

16. C. Conese and F. Maselli, "Use of multitemporal information to improve classification performance of TM scenes in complex terrain," *ISPRS J. Photogramm. Remote Sens.* **46**(4), 187–197 (1991), http://dx.doi.org/10.1016/0924-2716(91)90052-W.
17. C. A. O. Vieira and P. M. Mather, "An examination of the effectiveness of multi temporal classification," in *Proc. 26th Annual Conf. and Exhibition of the Remote Sensing Society*, University of Leicester, United Kingdom (2000).
18. D. Wang et al., "Application of multitemporal ENVISAT ASAR data to agricultural area mapping in the Pearl River Delta," *Int. J. Remote Sens.* **31**(6), 1555–1572 (2010), http://dx.doi.org/10.1080/01431160903475258.
19. V. Vapnik, *Statistical Learning Theory*, John Wiley, New York (1998).
20. A. R. S. Marçal et al., "Land cover update by supervised classification of segmented ASTER images," *Int. J. Remote Sens.* **26**(7), 1347–1362 (2005), http://dx.doi.org/10.1080/01431160412331291233.
21. M. Pal and P. M. Mather, "Support vector machines for classification in remote sensing," *Int. J. Remote Sens.* **26**(5), 1007–1011 (2005), http://dx.doi.org/10.1080/01431160512331314083.
22. M. Pal and G. M. Foody, "Feature selection for classification of hyperspectral data by SVM," *IEEE Trans. Geosci. Remote Sens.* **48**(5), 2297–2306 (2010), http://dx.doi.org/10.1109/TGRS.2009.2039484.
23. G. M. Foody and A. Mathur, "A relative evaluation of multiclass image classification by support vector machines," *IEEE Trans. Geosci. Remote Sens.* **42**(6), 1335–1343 (2004), http://dx.doi.org/10.1109/TGRS.2004.827257.
24. M. Pal, "Ensemble of support vector machines for land cover classification," *Int. J. Remote Sens.* **29**(10), 3043–3049 (2008), http://dx.doi.org/10.1080/01431160802007624.
25. L. Wang et al., "Settlement extraction in the North China Plain using Landsat and Beijing-1 multispectral data with an improved watershed segmentation algorithm," *Int. J. Remote Sens.* **31**(6), 1411–1426 (2010), http://dx.doi.org/10.1080/01431160903475332.
26. E. F. Vermote et al., "Second simulation of the satellite signal in the solar spectrum, 6S: an overview," *IEEE Trans. Geosci. Remote Sens.* **35**(3), 675–686 (1997), http://dx.doi.org/10.1109/36.581987.
27. R. G. Congalton and K. Green, *Assessing the Accuracy of Remotely Sensed Data: Principles and Practices*, Lewis Publishers, Florida (1999).
28. B. Tso and M. P. Mather, *Classification Methods for Remotely Sensed Data*, Taylor and Francis, London (2001).
29. G. M. Foody, "Classification accuracy comparison: hypothesis tests and the use of confidence intervals in evaluations of difference, equivalence and non-inferiority," *Remote Sens. Environ.* **113**(8), 1658–1663 (2009), http://dx.doi.org/10.1016/j.rse.2009.03.014.
30. G. M. Foody and A. Mathur, "A relative evaluation of multiclass image classification by support vector machines," *IEEE Trans. Geosci. Remote Sens.* **42**(6), 1335–1343 (2004), http://dx.doi.org/10.1109/TGRS.2004.827257.
31. T. Kavzoglu and I. Colkesen, "A kernel functions analysis for support vector machines for land cover classification," *Int. J. Appl. Earth Obs. Geoinform.* **11**(5), 352–359 (2009), http://dx.doi.org/10.1016/j.jag.2009.06.002.
32. C. Cortes and V. Vapnik, "Support-vector networks," *Mach. Learn.* **20**(3), 273–297 (1995), http://dx.doi.org/10.1007/BF00994018.
33. C. J. C. Burges, "A tutorial on support vector machines for pattern recognition," *Data Min. Knowl. Disc.* **2**(2), 121–167 (1998), http://dx.doi.org/10.1023/A:1009715923555.

Kun Jia is an assistant professor at the State Key Laboratory of Remote Sensing Science and College of Global Change and Earth System Science, Beijing Normal University, China. His current research interests include agriculture monitoring, crop type identification, and vegetation parameters estimation using remote sensing data.

Bingfang Wu is a professor at the Key Laboratory of Digital Earth Science and State Key Laboratory of Remote Sensing Science, Institute of Remote Sensing and Digital Earth, Chinese Academy of Sciences. His current research interests include remote sensing for agriculture, water resources, and ecosystem.

Qiangzi Li is a professor at the State Key Laboratory of Remote Sensing Science, Institute of Remote Sensing and Digital Earth, Chinese Academy of Sciences. His current research interests include crop acreage and yield estimation using remote sensing.